

# A23D-0194 Water vapor characteristics over tropical and subtropical oceans



\*Kaya Kanemaru<sup>1</sup>(kanemaru@satellite.hyarc.nagoya-u.ac.jp), Hirohiko Masunaga<sup>2</sup>

<sup>1</sup>Graduate School of Environmental Studies, Nagoya, Japan, <sup>2</sup>Hydrospheric Atmospheric Research Center, Nagoya, Japan

## 1. Background & Purpose

The hydrological cycle has important roles in maintaining the Earth's climate system. The purpose of this study is to explore the characteristics of water vapor with focus on climatological contrast between tropical and subtropical oceans.

## 2. Data & Method

Data acquired by the **Aqua** Advanced Microwave Scanning Radiometer for the Earth Observing System (**AMS**R-E), Atmospheric Infrared Sounder (**AIRS**) / Advanced Microwave Sounder Unit (**AMSU**) unit, the Tropical Rainfall Measuring Mission (**TRMM**) Precipitation Radar (**PR**), and the Quick Scatterometer (**QuikSCAT**) **SeaWinds** are analyzed for 7 years from October 2002 to September 2009 over 25° N to 25° S. All satellite data are projected onto 1° × 1° daily grid. In this study, **water vapor scale height**  $H_v$  is introduced to describe vertical moisture gradient (Fig.1), where

$$H_v \equiv \frac{W}{\rho_{v,s}} \quad (1)$$

$W$  and  $\rho_{v,s}$  are column water vapor (CWV) and surface water vapor density, respectively. Equation (1), the Clausius-Clapeyron relation, and the equation of state give

$$RH_0 \times H_v = \frac{W \times R_v \times T_s}{e_s(T_s)}, \quad (2)$$

where  $RH_0$ ,  $R_v$ ,  $T_s$ , and  $e_s(T_s)$  are surface air relative humidity, the gas constant for water vapor (= 461.5 J K<sup>-1</sup> kg<sup>-1</sup>), sea surface temperature (SST), and saturation vapor pressure for temperature  $T_s$ , respectively.

## 3.1. Result

The relationship between SST and CWV (Fig.2a) suggests that the ridge of the histogram roughly follows the diagnostic lines of (2) for low SSTs. For high SSTs, the ridge of the histogram crosses the diagnostic lines. On the other hand, the ridge of histogram between SST and  $\rho_{v,s}$  (Fig.2b) follows the iso- $RH_0$  lines over a range of SST. It suggests that the histogram between SST and CWV is not explained only by the variability of surface water vapor.  $RH_0$  stays nearly invariable at 80 % along the histogram ridge (Fig.2c). However, for higher SSTs, the histogram crosses  $H_v$  from 1500 to 2500 m (Fig.2d). This result suggests that the variability of CWV is explained not only by surface moisture but also by moisture vertical gradient.

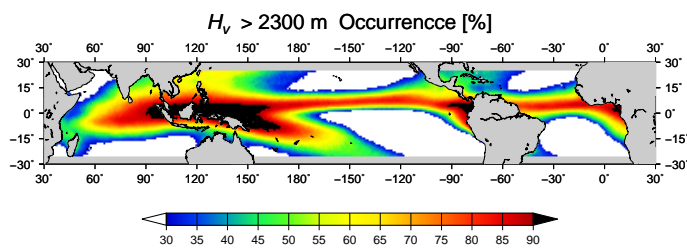


Fig.3 The occurrence of threshold of  $H_v > 2300$  m

The regions where  $H_v$  is larger than the climatological value of 2300 m are bound in tropical oceans (Fig.3).

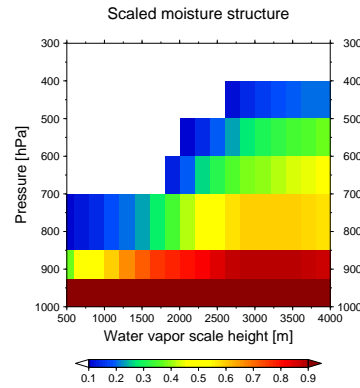


Fig.1 AIRS moisture profile, which is normalized by surface water vapor mixing ratio, sorted by  $H_v$ .

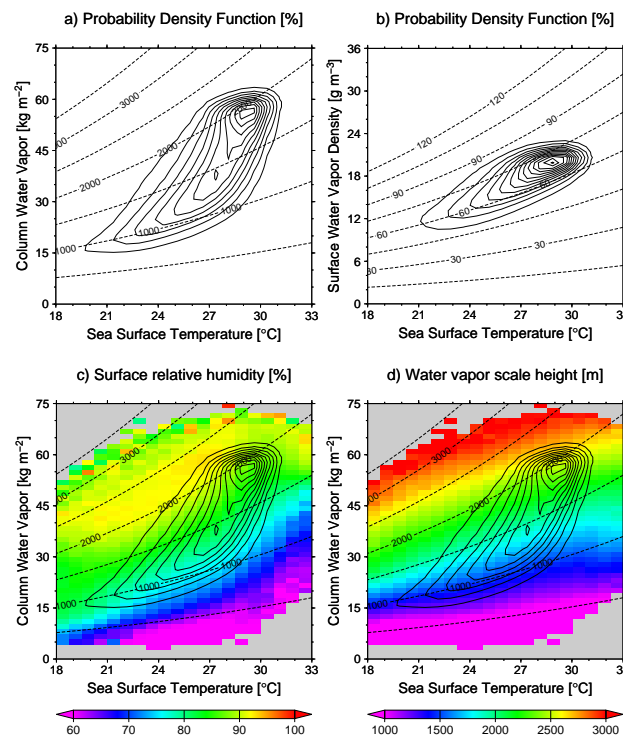


Fig.2 a) The joint probability density function of SST and CWV (solid line) and the diagnostic lines predicted from (2) (dash line). b) but, SST and  $\rho_{v,s}$ . c) distribution of  $RH_0$ . d) but,  $H_v$ .

## 3.2. Result

The relationship between SST and CWV is evaluated from a sensitivity analysis (Fig.4 left). From (2), the CWV sensitivity to SST is separated into

$$\frac{\partial \ln W}{\partial T_s} = \frac{\partial \ln RH_0}{\partial T_s} + \frac{\partial \ln H_v}{\partial T_s} + \frac{L_v - R_v T_s}{R_v T_s^2} \quad (3)$$

Figure 4 (right) shows each contribution in (3). The contribution of SST is almost constant as predicted by the Clausius-Clapeyron relation. For SSTs from 18 to 25 °C, the contribution of SST is dominate for the variability of CWV. For SSTs from 25 to 30 °C, on the other hand, the contributions of both SST and  $H_v$  are equally dominate. The contribution of  $RH_0$  is small for the variability of CWV.

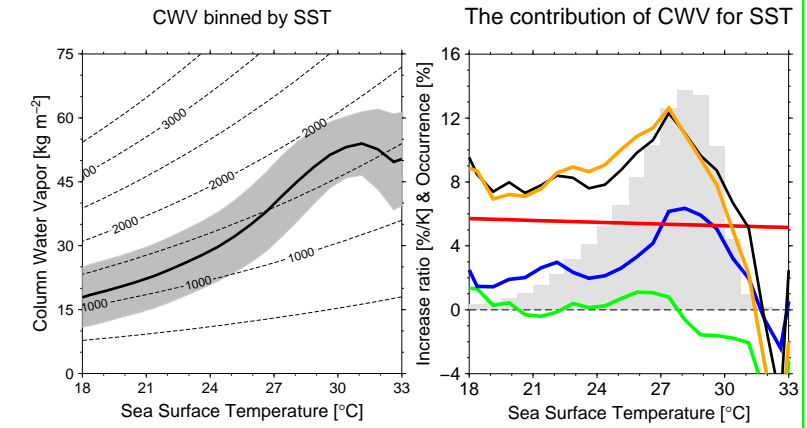


Fig.4 left) CWV binned by SST. The shading above and below each point is one standard deviation on averaged CWV. Thick line is averaged CWV. right) the contribution of increase ratio of CWV for SST (orange),  $RH$  (green),  $H_v$  (blue),  $T_s$  (red), and the sum of the 3 terms (black).

## 4. Discussion

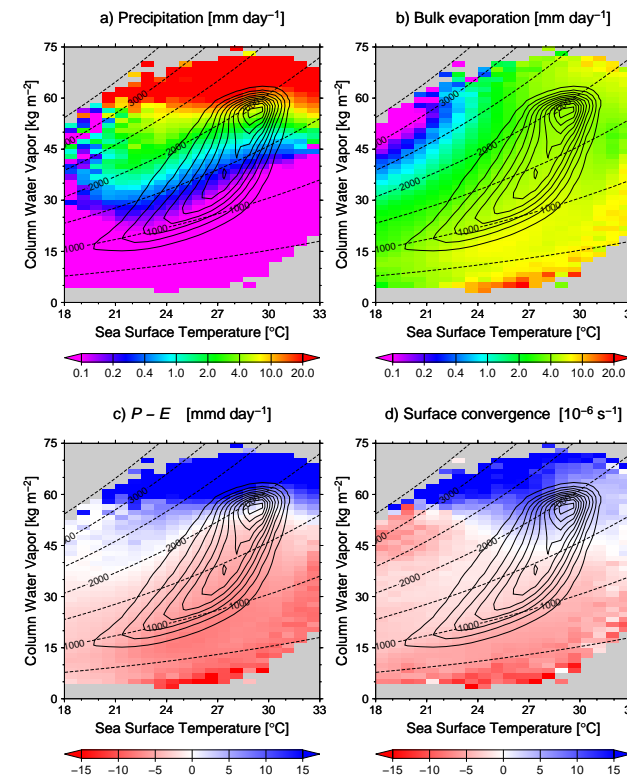


Fig.5 a) distribution of precipitation  $P$  between SST and CWV. b) a) but, bulk evaporation  $E$ . c) a) but,  $P - E$ . d) a) but, surface convergence.

The moisture budget and the dynamic field are discussed (Fig.5). Precipitation (Fig.5a) depends on CWV more strongly SST. On the other hands, bulk evaporation (Fig.5b) distributes relatively homogeneously compared to precipitation. Figure 5c shows the boundary between positive and negative  $P - E$  is about 50 mm of CWV. An excess and deficit of  $P - E$  is balanced with surface convergence and divergence (Fig.5d).

The following hypothesis is suggested from the present result. Surface divergence removes boundary layer moisture evaporated from the ocean and suppresses vertical moisture transport, which results in sharp vertical moisture gradient ( $H_v$  is small). On the other hand, surface convergence ventilates moisture from the boundary layer to the free troposphere, which results in steep vertical moisture gradient ( $H_v$  is large). The latter case accompanies deep convection as seen in Fig.6.

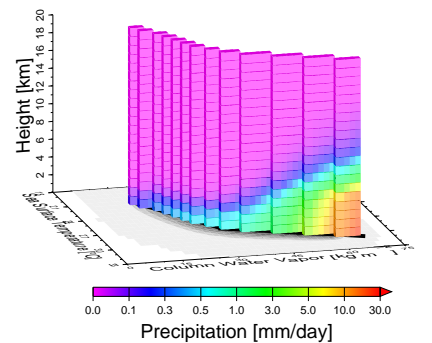


Fig.6 The vertical structure of precipitation.

## 5. Summary

The characteristics of water vapor over tropical and subtropical oceans are studied. Over subtropical oceans, the regional gradient of surface water vapor density mainly contributes to the variation of CWV. On the other hand, over tropical oceans, the variability of CWV is explained largely by water vapor scale height varying from one region to another. Surface relative humidity are climatologically homogeneous over tropical and subtropical oceans. The contrast between tropical and subtropical oceans may be explained in the context of regional water budget including vertical moisture transport through convection (Fig.7).

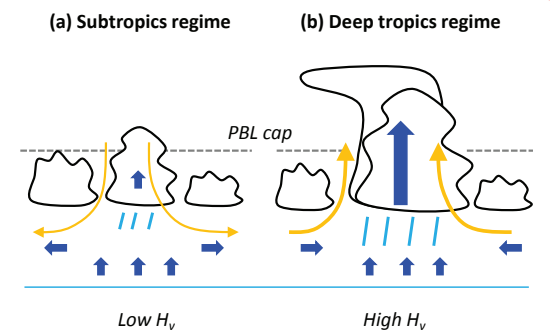


Fig.7 The schematics of characteristics of the moisture budget.